Available online at www.sciencedirect.com
SCIENCE DIRECT®
Earth and Planetary Science Letters 241 (2006) 65–79
EPSL
www.elsevier.com/locate/epsl

Primitive neon and helium isotopic compositions of high-MgO basalts from the Kerguelen Archipelago, Indian Ocean

Sonia Doucet [a,*], Manuel Moreira [a], Dominique Weis [b], James S. Scoates [b], André Giret [c], Claude Allègre [a]

[a] *Institut de Physique du Globe de Paris, Université Paris VII-Denis Diderot, CNRS UMR7579, Laboratoire de Géochimie et de Cosmochimie, 4 place Jussieu, 75252 Paris, Cedex 05, France*
[b] *Pacific Centre for Isotopic and Geochemical Research, Department of Earth and Ocean Sciences, 6339 Stores Road, University of British Columbia, Vancouver, Canada V6T1Z4*
[c] *Laboratoire Magmas et Volcans, CNRS-UMR 6524, Université Jean Monnet, 23 rue Paul, Michelon, 42023 St. Etienne, France*

Received 1 March 2005; received in revised form 19 October 2005; accepted 21 October 2005
Available online 28 November 2005

Abstract

The geochemical characteristics of mildly alkalic basalts (24–25 Ma) erupted in the southeastern Kerguelen Archipelago are considered to represent the best estimate for the composition of the enriched Kerguelen plume end-member. A recent study of picrites and high-MgO basalts from this part of the archipelago highlighted the Pb and Hf isotopic variations and suggested the presence of mantle heterogeneities within the Kerguelen plume itself. We present new helium and neon isotopic compositions for olivines from these picrites and high-MgO basalts (6–17 wt.% MgO) both to constrain the enriched composition of the Kerguelen plume and to determine the origin of isotopic heterogeneities involved in the genesis of Kerguelen plume-related basalts. The olivine phenocrysts have extremely variable $^{4}He/^{3}He$ compositions between MORB and primitive values observed in OIB (~90,000 to 40,000; i.e., R/R_a ~8 to 18) and they show primitive neon isotopic ratios (average $^{21}Ne/^{21}Ne_{ext}$ ~0.044). The neon isotopic systematics and the $^{4}He/^{3}He$ ratios that are lower than MORB values for the Kerguelen basalts clearly suggest that the Kerguelen hotspot belongs to the family of primitive hotspots, such as Iceland and Hawaii. The rare gas signature for the Kerguelen samples, intermediate between MORB and solar, is apparently inconsistent with mixing of a primitive component with a MORB-like source, but may result from sampling a heterogeneous part of the mantle with solar $^{3}He/^{22}Ne$ and with a higher $(U,Th)/^{3}He$ ratio compared to typically high R/R_a hotspot basalts such as those from Iceland and Hawaii.

Keywords: helium and neon isotopes; Kerguelen plume; high-MgO basalts; olivine; mantle

1. Introduction

The Kerguelen Archipelago (Fig. 1) is located in the Indian Ocean, 1200 km to the southwest of St. Paul Island on the Southeast Indian Ridge (SEIR) and represents the subaerial expression of the last 40 Ma of Kerguelen mantle plume-related volcanic activity. Kerguelen plume activity has been recorded over the last 132 Ma [1–17] and the relative position of the Kerguelen hotspot compared to continental margins and Indian Ocean ridge has changed considerably during this long period of time. These variations are reflected in the variable isotopic geochemistry of Kerguelen plume-related basalts. In particular, there is no geochemical

* Corresponding author.
E-mail address: sonia.mo.doucet@wanadoo.fr (S. Doucet).

0012-821X/$ - see front matter © 2005 Elsevier B.V. All rights reserved.
doi:10.1016/j.epsl.2005.10.025

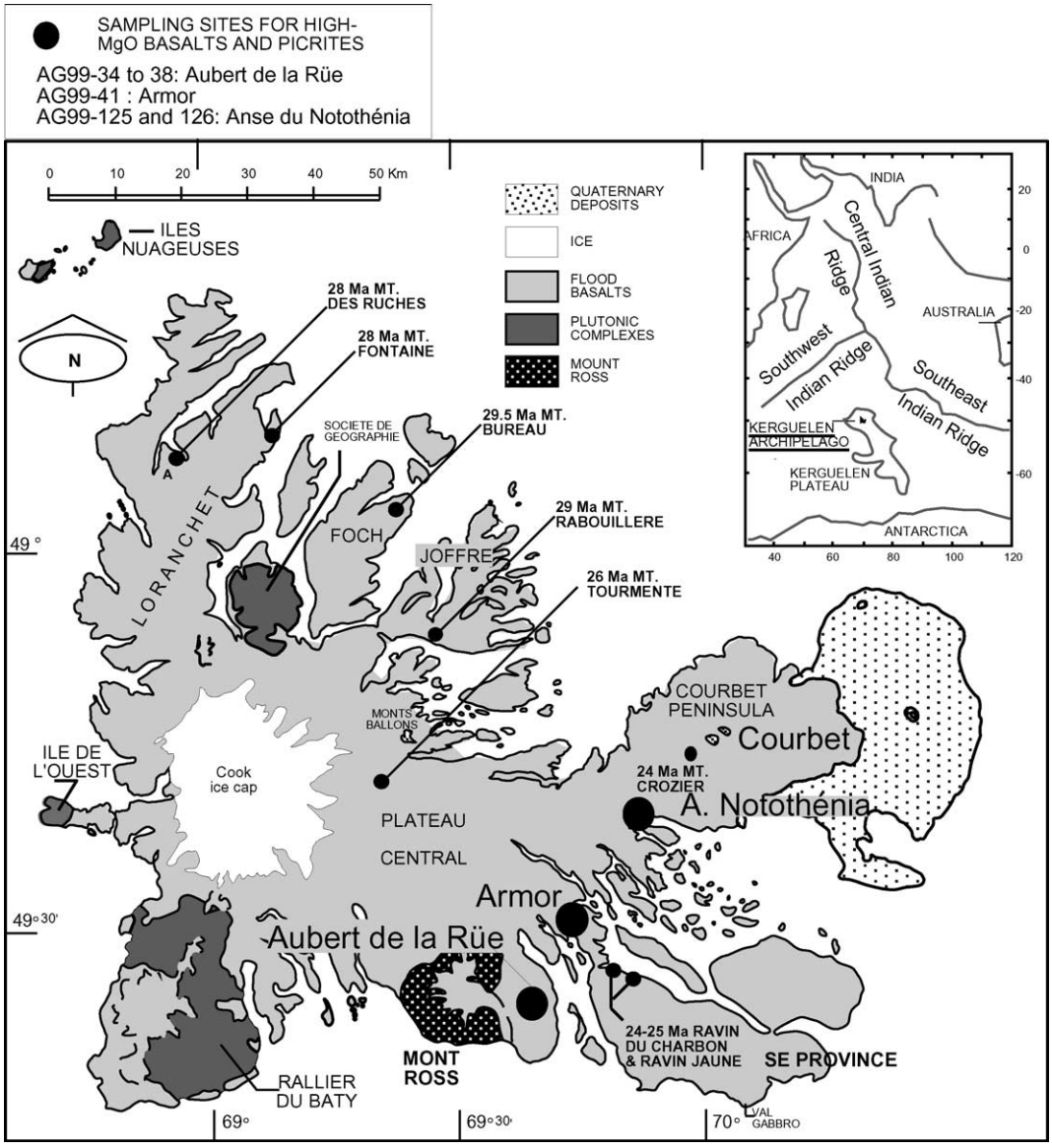

Fig. 1. Simplified geological map of the Kerguelen Archipelago after [78] showing the distribution of flood basalts (85% of the surface area), plutonic complexes (5%) and Quaternary deposits (10%). The locations of basaltic sections that have been studied to date are labeled with solid black circles and the sample sites for the picrites and high-MgO basalts in this study are indicated by the large filled circles. Complete descriptions of the samples are provided in [14]. Inset in the figure shows a schematic map of the Indian Ocean with the location of the Kerguelen Archipelago.

evidence for continental contamination in the 29–24 Ma Kerguelen Archipelago lavas that formed far away from continental margins. In these lavas, the role of a mid-ocean ridge basalt (MORB)-like source component is identified in early tholeiitic–transitional basalts (29 Ma) that formed closer (about 200 km) to the SEIR-axis (e.g., [13–16,18–20]). This is followed by a decreasing contribution of the SEIR–MORB-like source with decreasing eruption age in the geochemistry of the Kerguelen Archipelago basalts. Finally, the youngest basalts collected on the archipelago (24–25 Ma), which erupted when the archipelago was about 400 km away from the ridge axis, show little to no significant contribution of a MORB-like source. Mildly alkalic basalts (24–25 Ma) erupted in the southeastern Kerguelen Archipelago (Fig. 1) have limited Pb–Sr–Nd–Hf isotopic variations that are considered as the best estimates for the composition of the enriched Kerguelen plume end-member [20–23]. Doucet et al. [14] showed that MgO-rich rocks from this part of the

archipelago are characterized by significant Pb and Hf isotopic variations that may reflect the presence of discrete heterogeneities within the Kerguelen mantle plume source itself. Alternatively, these variations could reflect contamination of the parental magmas by the overlying Kerguelen Plateau, although no obvious geochemical evidence to date is supportive of such a hypothesis. Additional information is thus required to better characterize the nature of discrete heterogeneities within the mantle source of Kerguelen plume-derived basalts.

Helium has two stable isotopes, ^{3}He and ^{4}He. ^{3}He has mainly a primordial origin, whereas ^{4}He is produced during radioactive decay of U and Th. The helium systematics in oceanic basalts suggest the existence of different reservoirs in the Earth's mantle [24,25]. The ^{4}He/^{3}He ratio for MORB has been shown to be relatively constant with a value of $90{,}000 \pm 10{,}000$ (or $R/R_a = 8 \pm 1$, where R and R_a are ^{3}He/^{4}He ratios for the sample and air, respectively). Oceanic island basalts (OIB) show variable ^{4}He/^{3}He ratios between extremely low ratios of ~15,000 ($R/R_a = 50$) to ratios more radiogenic than the mean MORB value (>150,000, $R/R_a < 5$) [25–32]. These observations were interpreted as reflecting the existence of a layered mantle, with the MORB source being a degassed reservoir and the source of low ^{4}He/^{3}He mantle plumes being less degassed [29,33,34]. The origin of hotspots having more radiogenic ^{4}He/^{3}He than MORB is still debated, but they are generally attributed to mantle plumes sampling recycled oceanic lithosphere and/or sediments [26,31,35]. An alternative explanation for these radiogenic helium ratios is helium degassing, followed by radiogenic production and/or crust assimilation [34,36,37].

Neon has three isotopes, ^{20}Ne, ^{21}Ne, and ^{22}Ne. ^{21}Ne is produced by nucleogenic reactions ^{18}O(α,n)^{21}Ne and ^{24}Mg(n,α)^{21}Ne, which are related to U and Th decay. Nucleogenic production of ^{21}Ne is therefore related to the production of radiogenic helium, and the production ratio ^{4}He/^{21}Ne is estimated at 2.2×10^7 in the mantle [38]. MORB samples are linearly distributed in a three neon isotope diagram (^{20}Ne/^{22}Ne vs. ^{21}Ne/^{22}Ne) [39] and are characterized by both higher ^{20}Ne/^{22}Ne and ^{21}Ne/^{22}Ne ratios than the atmospheric values of 9.8 and 0.029, respectively. The linear distribution of samples in a three neon isotope diagram is generally interpreted as reflecting air contamination of a magma having ^{20}Ne/^{22}Ne higher than 12.5 (e.g., solar-like; the solar wind value being 13.8 [40]). Note that the origin of the difference observed between atmospheric ^{20}Ne/^{22}Ne of 9.8 and mantle ^{20}Ne/^{22}Ne>12.5 is commonly attributed to a neon loss, with mass fractionation, during either the phase T-Tauri of the sun or to the large impact that created the moon [49,50]. Similar to MORB samples, OIB samples show higher ^{20}Ne/^{22}Ne and ^{21}Ne/^{22}Ne than atmospheric values. In addition, OIB are systematically characterized by lower ^{21}Ne/^{22}Ne ratios for a given ^{20}Ne/^{22}Ne ratio compared to MORB [41–48]. These neon systematics again suggest the existence of at least two distinct reservoirs in the mantle: one having low ^{22}Ne content and the other one being much less degassed [33], thus confirming the helium isotopic systematics of oceanic basalts.

Because of the scarcity of high-MgO basalts on the Kerguelen Archipelago, only a few rare gas analyses are available for this site. Previous measurements on Kerguelen xenoliths [51–53] and on Kerguelen basalts [K. Nicolaysen, unpublished data] have shown important helium isotopic variations with ^{4}He/^{3}He ratios between 145,000 and 36,000 (R/R_a between 5 and 20). Only a few values of xenoliths and basalts reach the moderate to high R/R_a of 12 to 20 (^{4}He/^{3}He ~60,000 and 36,000), recorded in some OIB such as Iceland and Hawaii (e.g., [41–43,46,54,55]). The majority of helium isotopic ratios determined from Kerguelen basalts and xenoliths to date are close to the mean MORB ratio (^{4}He/^{3}He = $90{,}000 \pm 10{,}000$ or $R/R_a \approx 8 \pm 1$). We present in this study new helium and neon isotopic compositions for olivines from eight high-MgO basalts and picrites (6–17 wt.% MgO) collected in the southeastern Kerguelen Archipelago. These compositions are used to determine the isotopic characteristics of the enriched component of the Kerguelen mantle plume and constrain the origin of isotopic variations observed in the high-MgO basalts and picrites from the Kerguelen Archipelago [14].

2. Samples and analytical procedure

Blocks and boulders of high-MgO basalts and picrites were sampled from the southeastern Kerguelen Archipelago area during the CartoKer field mission in Nov–Dec 1999 (Fig. 1) and were selected on the basis of the presence and abundance of olivine phenocrysts. A detailed description of the location and the origin of these samples is provided in [14]. Both rounded and euhedral olivines are present in the samples. The average core compositions for the olivine phenocrysts is $\approx Fo_{80}$ and the most Mg-rich olivine (Fo_{87}) is from sample AG99-34 (see olivine core and rim compositions in [14]). Only two samples (AG99-34 and AG99-36) provided enough material for distinct olivine phenocryst populations to be separated and analyzed. In

Table 1
Helium and neon abundances and isotopic ratios in olivine aliquots from eight Kerguelen Archipelago basalts

A. Crushing experiments on olivines phenocrysts

Sample	Machine	Olivine material	Weight (g)	Crushing strokes	^{4}He (10^{-9}) (cm^3 STP/g)	^{4}He/^{3}He	R/R_a	1σ	^{22}Ne (10^{-12}) (cm^3 STP/g)	^{20}Ne/^{22}Ne	1σ	^{21}Ne/^{22}Ne	1σ	^{21}Ne/^{22}Ne$_{ext}$
AG99-34 a	ARESIBO	Light green	0.90	200	3.6	53128	13.6	0.9	0.165	9.84	0.14	0.0292	0.0021	
AG99-34 b	ARESIBO	Light green	1.95	400	4.3	61589	11.7	0.5	0.495	10.25	0.05	0.0301	0.0007	0.038
AG99-34 c	ARESIBO	Brown olive	0.94	600	1.5	41218	17.5	2.5	0.447	9.85	0.10	0.0290	0.0007	
AG99-34 d	WHOI	Light green	0.29		2.5	68945	10.5	0.3						
AG99-35 a	ARESIBO	Brown olive	0.78	200	6.5	79996	9.0	0.6	1.158	10.19	0.08	0.0303	0.0009	0.043
AG99-35 b	ARESIBO	Brown olive	2.06	325	8.7	79939	9.0	0.3	1.515	10.42	0.05	0.0311	0.0004	0.042
AG99-36 a	ARESIBO	Light green	0.85	200	4.5	81621	8.9	0.9	0.387	10.14	0.11	0.0280	0.0013	
AG99-36 b	ARESIBO	Light green	1.65	600	4.8	74465	9.7	0.5	0.493	10.42	0.07	0.0319	0.0005	0.047
AG99-36 c	ARESIBO	Light green	2.12	400	7.4	69913	10.3	0.4	0.909	10.34	0.06	0.0320	0.0008	0.052
AG99-36 d	ARESIBO	Brown olive	1.28	700	6.4	65094	11.1	0.5	0.440	10.30	0.07	0.0299	0.0011	0.036
AG99-36 e	WHOI	Light green	0.29		0.5	87454	8.3	1.0						
AG99-37	ARESIBO	Brown olive	1.26	550	4.9	91461	7.9	0.8	0.681	10.66	0.07	0.0328	0.0007	0.047
AG99-38 a	ARESIBO	Brown olive	1.24	550	16.0	73206	9.9	0.2	0.412	10.55	0.07	0.0312	0.0009	0.041
AG99-38 b	WHOI	Brown olive	0.30		16.6	75588	9.6	0.1						
AG99-41	ARESIBO	Brown olive	1.35	445	20.0	67213	10.8	0.1	1.590	10.33	0.04	0.0313	0.0005	0.046
AG99-125 a	ARESIBO	Brown olive	0.89	300	5.1	52326	13.8	.8	1.897	9.83	0.05	0.0279	0.0008	
AG99-125 b	ARESIBO	Brown olive	1.27	455	6.3	48202	15.0	0.3	1.240	10.24	0.05	0.0303	0.0005	0.041
AG99-126 a	ARESIBO	Brown olive	0.86	350	3.8	58972	12.3	1.4	0.692	10.04	0.09	0.0289	0.0009	
AG99-126 b	ARESIBO	Brown olive	1.55	520	3.3	50492	14.3	0.4	2.580	9.95	0.03	0.0297	0.0003	0.048
AG99-126 c	WHOI	Brown olive	0.24		1.5	66840	10.8	0.55						

B. Heating experiments on olivines powders (remaining from crushing)

Heating	Machine	Olivine material	Weight (g)	T reached (°C)	^{4}He(10^{-9}) (cm^3 STP/g)	^{4}He/^{3}He	R/R_a	1σ
AG99-34	ARESIBO	Light green	0.36	1000–1100	8.25			
AG99-35	ARESIBO	Brown olive	0.38	1000–1100	30.00	475913	1.5	1.1
AG99-36	ARESIBO	Light green	0.36	1000–1100	7.90	50800	14.2	3.0
AG99-37	ARESIBO	Brown olive	0.38	1000–1100	14.72	28915	25.0	2.3
AG99-38	ARESIBO	Brown olive	0.37	1000–1100	9.36	25684	28.1	3.6
AG99-41	ARESIBO	Brown olive	0.37	1000–1100	13.03	124774	5.8	2.5

Helium and neon concentrations and isotopic compositions for olivines from high-MgO basalts on the Kerguelen Archipelago. A. Helium and neon concentrations and isotopic composition of gas extracted by crushing. B. Helium concentrations and isotopic compositions determined by heating experiments on olivine powders (remaining from crushing experiments). WHOI means Woods Hole Oceanographic Institution. ARESIBO is the name of mass spectrometer used at IPGP (ARESIBO 1). R/R_a: R is the value of ^{3}He/^{4}He measured in the sample; R_a is the ^{3}He/^{4}He atmospheric ratio (1.384×10^{-6}). ^{21}Ne/^{22}Ne$_{ext}$ is the value of ^{21}Ne/^{22}Ne "extrapolated", which is the value of ^{21}Ne/^{22}Ne expected when removing air contamination ^{21}Ne/^{22}Ne$_{ext}$=(^{20}Ne/^{22}Ne$_{solar}$−^{20}Ne/^{22}Ne$_{air}$)×(^{21}Ne/^{22}Ne$_{measured}$−^{21}Ne/^{22}Ne$_{air}$)/(^{20}Ne/^{22}Ne$_{measured}$−^{20}Ne/^{22}Ne$_{air}$)+^{21}Ne/^{22}Ne$_{air}$ with ^{20}Ne/^{22}Ne$_{solar}$=13.8, ^{20}Ne/^{22}Ne$_{air}$=9.8, and ^{21}Ne/^{22}Ne$_{air}$=0.029.

these samples, the most abundant population is characterized by pure light green olivine crystals containing few oxide inclusions and no visible melt inclusions. The less abundant population in samples AG99-34 and AG99-36 is characterized by typical brown olive crystals containing many melt and fluid inclusions. These crystals are typically rounded or resorbed, which suggests that they were in disequilibrium with the melt. Despite the fact that direct analysis of phenocrysts was not done for this study, analyses of sample AG99-34 provided in [14] show that euhedral crystals are slightly more Mg-rich (average Fo_{84}) than resorbed and rounded crystals (average Fo_{80}), which confirms the presence of two populations. We analyzed the two populations separately in order to investigate whether these olivines were formed from magmas with isotopically distinct sources.

Noble gas analyses in subaerial lavas are generally done with olivines that include fluid or melt inclusions that themselves contain mantle-derived gases. Cosmogenic helium and/or neon, produced by interaction of secondary neutrons with the major elements of olivine, are located within the matrix of the minerals [56–59]. The more appropriate analytical method for extracting the mantle signal from this material thus consists in crushing the olivines under high vacuum. Cosmogenic helium can then be released by heating the powder. However, some cosmogenic helium (up to 25%) can be extracted during the crushing process, especially in old samples that have been exposed for a long time to cosmic rays [60,61]. Therefore, special attention needs to be given to the interpretation of measured primitive helium isotopic ratios in samples with a long exposure history to cosmic rays, such as the relatively "old" MgO-rich rocks from the Kerguelen Archipelago (24–29 Ma [62]).

The rocks were crushed to approximate the olivine phenocryst grain sizes (≤2 mm) and about 0.7 to 2 g of olivine phenocrysts were handpicked from this material. Olivines were cleaned with 7N HF, ethanol and acetone. The samples were loaded in a crusher and baked overnight at ~150 °C under vacuum using a turbo-molecular pump. The samples were crushed using a magnetic ball moved with a magnet. The number of strokes that were done to complete the crushing procedure is reported in Table 1. The gas extracted from this step was purified with a hot Ti-getter and a SAES-getter at room temperature. Noble gases were trapped at a temperature of 10 K on charcoal using a cryogenic system. Helium was separated from neon at 35 K and neon from the other noble gases at 75 K. These gases were introduced successively into the ARESIBO I glass mass spectrometer. The analytical procedure was performed using a new fully automated line with low helium and neon blanks ($^4He = 4\times10^{-10}$ and $^{22}Ne = 1.5\times10^{-13}$ cm^3 STP).

Duplicate analyses of the samples were carried out when sufficient quantities of olivine were available. This was the case for samples AG99-34, -35, -36, -125, and -126. In addition, four samples were also duplicated for helium isotopic analysis at the Woods Hole Oceanographic Institution (WHOI) by M.D. Kurz (AG99-34, -36, -38, and -126). Gas extraction was also done by crushing these samples. The analytical procedure is associated with low helium blanks ($^4He = 3$ to 5×10^{-11} cc STP He). Note that the size of olivine samples analyzed at WHOI was smaller compared to those analyzed at the Institut de Physique du Globe de Paris (IPGP) (<1 and >1 mm, respectively) because only a small amount of material was available at this stage.

For six samples (AG99-34, -35, -36, -37, -38, and -41), the gas present in the olivine matrix (i.e., in the powder remaining from the crushing procedure, ~μm size powder) was extracted by heating at ~1000 °C for 30 min. The heating procedure was done in a separate stainless steel tube and blanks measured between each extraction were as low as blanks measured between crushing experiences. The cosmogenic and/or radiogenic helium located in the olivine matrix was then analyzed using the same analytical procedure as that used for crushing. The heating temperature (~1000 °C) was below the melting point for pure forsterite olivine (1850 °C). However, considering the size of the grains (~1 μm), a diffusion coefficient of helium at 1000 °C of D ~10^{-10} cm^2/s [63], complete extraction of the helium can be achieved after a time $t = x^2/D$ of ~100 s.

3. Results

3.1. Helium results

Helium results are presented in Table 1. Helium isotopic compositions are represented as a function of ^{4}He concentration on Fig. 2A for results obtained by crushing only. The quality of duplicate analyses for helium isotopic compositions and for ^{4}He concentrations that result from the three different procedures at IPGP and at WHOI by crushing, and at IPGP by heating, are shown on Fig. 2B and C.

3.1.1. Crushing results

Helium concentrations vary from 0.5 to 20×10^{-9} cm^3 STP/g (Fig. 2A). Isotopic and concentration results

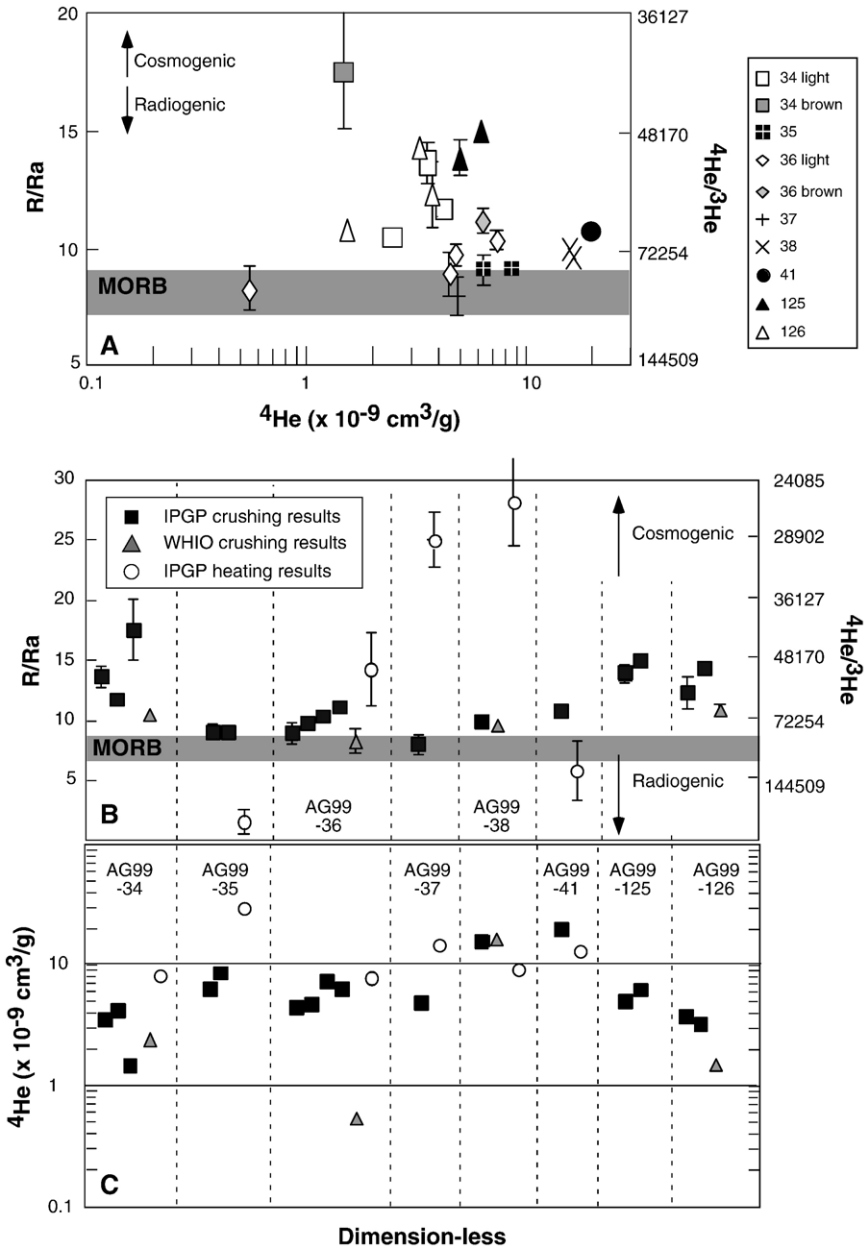

Fig. 2. A. $^4He/^3He$ (and corresponding R/Ra) vs. $^4He/^3He$ determined for olivine phenocrysts from the Kerguelen Archipelago by the crushing extraction procedure only. B and C. All results (B. $^4He/^3He$, and C. ^4He concentrations) determined for duplicates made at IPGP (by crushing: black squares, and heating extraction procedure: white circles) and at WHOI (crushing procedure: grey triangles). Note: (1) important variations of $^4He/^3He$=90,000 to 25,000 (i.e., $R/R_a \approx 8$ to 29, typical values from MORB to OIB), (2) differences between two populations of olivine phenocrysts (3) significant differences between results obtained by heating experiments vs. crushing experiments, and (4) duplicates made at WHOI are systematically characterized by higher $^4He/^3He$ than those analyzed at IPGP, when different.

for samples AG99-35, -38, and -125 are reproducible within 1σ (Fig. 2B and C). For samples AG99-36 and AG99 -126, duplicates are reproducible at 2σ, except for ^4He concentrations obtained at WHOI, which are particularly low (0.5 and 1.5×10^{-9} cm^3 STP/g, respectively). Finally, for sample AG99-34, two duplicates are reproducible at 2σ for isotopic and ^4He concentrations, whereas the other two duplicates both have lower ^4He concentrations. For these latter two samples, the samples duplicated at WHOI have slightly lower R/R_a and the sample measured at IPGP has higher R/R_a, but is affected by a large 1σ error.

Except for sample AG99-38, the other three duplicates analyzed at WHOI on smaller grain size (grey triangles on Fig. 2B and C) show lower ^{4}He concentrations and R/R_a values than those analyzed at IPGP. These duplicates, despite being characterized by lower values of ^{4}He, are reproducible with the IPGP helium isotopic values at 2σ. Finally, important variations of helium isotopic compositions can be observed (Fig. 2B), from typical MORB values (90,000 or $R/R_a \approx 8$; e.g., sample AG99-37) to a more primitive signature of 41,200 ($R/R_a = 17.5 \pm 2.5$; e.g., sample AG99-34).

3.1.2. Heating results

Helium concentrations vary from 7.9 to 30×10^{-9} cm^3 STP/g (Fig. 2A). This clearly suggests that the heating procedure allowed for degassing of the powder at ~1000 °C (cf., Section 2). The ^{4}He/^{3}He ratios vary between very low ratios (25,700 for sample AG99-38) and extremely radiogenic values (475,900 or $R/R_a = 1.5$; sample AG99-35) (Fig. 2B). Sample AG99-34 did not show any measurable ^{3}He, but rather shows a relatively high ^{4}He content suggesting a radiogenic component in the olivine matrix.

3.2. Neon results

Neon contents and isotopic ratios are given in Table 1. Neon concentrations range from 0.17 to 2.6×10^{-12} cm^3 STP/g. ^{20}Ne/^{22}Ne and ^{21}Ne/^{22}Ne values show clear anomalies compared to air and they are between atmospheric values of 9.8 and 0.029, respectively, and values of up to 10.66 ± 0.07 and 0.0328 ± 0.0007 (sample AG99-37), respectively. Data from this study are reported in Fig. 3 together with the MORB line [39], the solar wind composition [40], and the Loihi and Iceland lines [46,48]. Also shown are the results determined for Kerguelen Archipelago xenoliths [52]. All of the compositions determined in this study are distributed on a line, which is characterized by an intermediate slope between the MORB and Iceland lines, near the Loihi line.

4. Discussions

Below, we (1) discuss the origin of helium isotopic ratio variability observed within one single sample and between the different Kerguelen Archipelago high-MgO basalts, and (2) evaluate the source of the Ker-

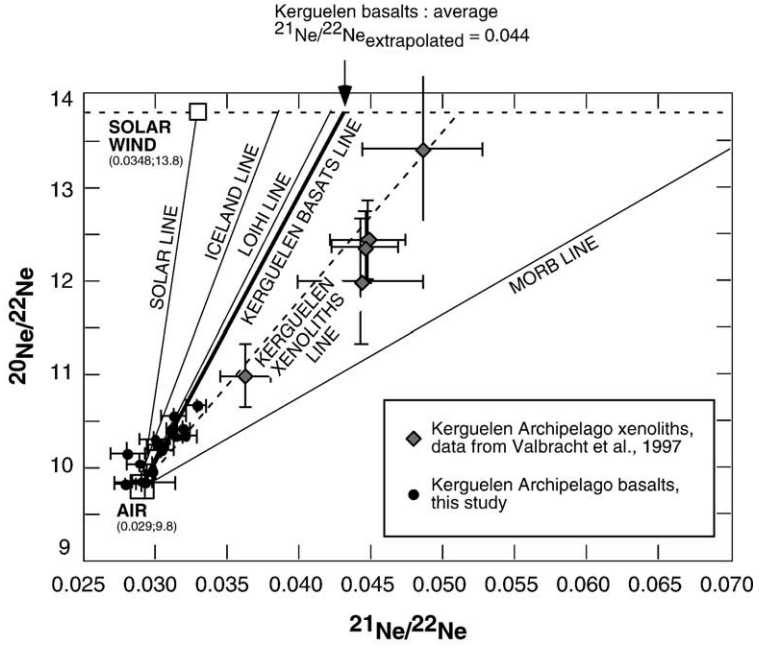

Fig. 3. ^{20}Ne/^{22}Ne vs. ^{21}Ne/^{22}Ne triplot of high-MgO basalts from the Kerguelen Archipelago. Neon isotopic results are reproducible within error. The high-MgO basalts and picrites form a linear trend that is characterized by an intermediate slope between the Iceland and MORB lines with an average ^{21}Ne/^{22}Ne$_{ext}$ value of 0.044, thus indicating that gas present in the olivine melt and fluid inclusions has a primitive origin (low ^{21}Ne/^{22}Ne extrapolated relative to MORB). Note that the linear distribution of the samples is interpreted as a binary mixture between the air and a mantle component with a constant ^{20}Ne/^{22}Ne of 13.8. The Kerguelen Archipelago xenoliths previously analyzed are also reported with the corresponding line, which is intermediate between the Kerguelen basalts and the MORB lines [52]. The MORB line is that defined by [39]. The solar line between the atmospheric composition (0.029, 9.8) and solar estimates (0.033, 13.8) are from [79].

guelen Archipelago high-MgO basalts and picrites in light of the helium–neon isotopic systematics, together with previously published Hf–Nd–Pb–Sr isotopic compositions for these MgO-rich rocks [14].

4.1. Helium isotopic variations

Three samples show large variations of helium isotopic ratios for olivines obtained by the crushing procedure (AG99-34, AG99-36, and AG99-126; Fig. 2B). $^4He/^3He$ ratios are between $41{,}200 \pm 6100$ and $69{,}000 \pm 4100$ for sample AG99-34, between $65{,}100 \pm 3000$ and $87{,}500 \pm 10{,}500$ for sample AG99-36, and between $50{,}500 \pm 1300$ and $66{,}900 \pm 3400$ for sample AG99-126. One possibility for explaining such variability within single basaltic samples is that this reflects the natural variability of olivine magmatic signatures within a sample. The observation of different olivine populations in the majority of the samples (cf., Section 2) supports this hypothesis. In particular, in samples AG99-34 and AG99-36, for which two distinctive populations were abundant enough to be analyzed separately, most "primitive" helium isotopic compositions (higher R/R_a and lower $^4He/^3He$) are recorded in the population characterized by brown olivine crystals that contain many melt and fluid inclusions ($^4He/^3He = 41{,}200 \pm 6100$ and $65{,}100 \pm 3000$ for samples AG99-34 and AG99-36, respectively). In contrast, the other three analyses of sample AG99-36, which all correspond to light green olivine phenocrysts, are reproducible within 1σ error. Note that all of the duplicate values for sample AG99-125 are reproducible. This particular sample has already been highlighted, because it represents a high-MgO sample from the Kerguelen Archipelago in which the olivine phenocrysts are compositionally in equilibrium with the basaltic melt (i.e., no substantial olivine accumulation apparently occurred for this sample) [14]. Good reproducibility in this case may thus reflect the homogeneity of the olivine population in sample AG99-125.

The olivine phenocryst populations analyzed at IPGP were approximately twice the size of the olivine phenocrysts analyzed in WHOI (cf., Section 2). We observe large geochemical variations between duplicates of sample AG99-34 made on smaller grains ($^4He/^3He \approx 69{,}000 \pm 1900$, $R/R_a = 10.5 \pm 0.3$; WHOI) and larger grains ($^4He/^3He \approx 61{,}600 \pm 2500$; $R/R_a = 11.7 \pm 0.5$; IPGP). Similar observations are made for sample AG99-36 on smaller grains ($^4He/^3He \approx 87{,}500 \pm 10{,}500$, $R/R_a = 8.3 \pm 1.0$; WHOI) and larger grains ($^4He/^3He \approx 70{,}000 \pm 2600$; $R/R_a = 10.3 \pm 0.4$; IPGP) and more important variations are observed for sample AG99-126 on smaller grains ($^4He/^3He \approx 67{,}000 \pm 3400$, $R/R_a = 10.8 \pm 0.6$; WHOI) and larger grains ($^4He/^3He \approx 50{,}500 \pm 1300$; $R/R_a = 14.3 \pm 0.4$; IPGP). These differences between results obtained in the two laboratories are consistent with similar observations previously made in Hawaiian lavas by Kurz et al. [64] on the effect of grain size on helium isotopic compositions. These authors interpret the differences in isotopic compositions of small grains and phenocrysts as reflecting the natural variability within phenocryst populations. In contrast to the observations made for samples AG99-34, -36, and -126, isotopic ratios and ^4He concentrations analyzed for sample AG99-38 at IPGP and WHOI are perfectly reproducible, which clearly indicates good interlaboratory reproducibility (Table 1; Fig. 2B and C). The large variations observed in the other samples may thus reflect the natural variability of the olivine phenocryst trace element and isotopic compositions within such basaltic samples. However, below we examine other processes that could potentially generate isotopic variability.

Extraction of cosmogenic or radiogenic helium from the matrix during crushing may also have disturbed the magmatic signal leading to the isotopic variations observed for the Kerguelen samples. The samples analyzed in this study are relatively old (~25 Ma), and may have been exposed to cosmic rays for a long time and thus probably contain substantial amounts of cosmogenic helium in the matrix. Radiogenic helium may also be present in the olivine matrix due to alpha implantation from the relatively U–Th-rich basalt during this period of time. This is illustrated by heating experiments that show significant quantities of radiogenic and cosmogenic helium within the matrix (Table 1 and white circles on Fig. 2B and C). It has been shown that up to a few percent of helium present in the matrix can be extracted during crushing depending on the quality of the crushing procedure [60,61]. This is an important process to consider because the Kerguelen samples are generally poor in mantle-derived helium (~$2–3 \times 10^{-9}$ cm^3 STP/g) and even a small contribution of helium present in the matrix may thus significantly influence the total helium signal for the sample. Therefore, helium isotopic variations observed in duplicate analyses maybe due either to 1) natural heterogeneity of magmatic helium compositions, or 2) distinct relative contributions of cosmogenic, radiogenic and magmatic helium during each analytical procedure. Detailed analysis of the results obtained by crushing and subsequent heating allows us to place qualitative constraints on the distinct relative contribu-

tion of cosmogenic, radiogenic and magmatic helium during the analytical procedure. For example, helium isotopic variations and ^{4}He concentration variations (with constant ^{3}He concentration) observed for AG99-34 light olivines (AG99-34 a and b; Table 1) might be interpreted as reflecting the increasing contribution of radiogenic helium due to a more efficient crushing process (strokes 200 to 400; Table 1). Indeed, the powder of AG99-34 left after crushing clearly contains a radiogenic component in the matrix that was extracted by heating (^{4}He$=8\times10^{-9}$ cm^3 STP/g; no detectable ^{3}He). If we consider that the composition of AG99-34a represents a magmatic composition (i.e., without any contribution of post-magmatic radiogenic helium), and that the helium isotopic variations in sample AG99-34 from $R/R_a=13.6\pm0.9$ to 11.7 ± 0.5 (samples a and b; Table 1) are due to an increasing contribution of radiogenic helium, then this indicates that the additional 200 strokes allowed for the extraction of 16% of the radiogenic ^{4}He ((4.3–3.6)/4.3×100), which is 8.5% of the ^{4}He measured in the AG99-34 matrix while heating the sample. Note that this estimation represents a maximum contribution because the analytical uncertainty is not considered in this rough estimation. This seems a reasonable percentage [60]. If post-magmatic radiogenic helium disturbed the magmatic signal, then the R/R_a signature of 11.7 ± 0.5 for sample AG99-34 (value of AG99-34 associated with the smallest error bar) represents a minimum value for the magmatic composition, which is consistent with a primitive origin. Similarly, we can compare the variable compositions recorded in sample AG99-36. In this case, heating results for the sample highlight the presence of cosmogenic ^{3}He together with radiogenic ^{4}He in the olivine matrix ($R/R_a=14.2$; ^{4}He$=7.9\times10^{-9}$ cm^3 STP/g). When comparing the compositions of AG99-36a and AG99-36c, increasing R/R_a from 8.9 ± 0.9 to 10.3 ± 0.4 might be related to an increasing cosmogenic contribution (and to a lesser extent, a radiogenic contribution) due to more efficient crushing (200 to 400 strokes). In this case, we roughly estimate a maximum contribution of cosmogenic helium of 33% of the ^{3}He measured in the AG99-36 matrix while heating the sample. Such proportions appear particularly elevated considering the duration of the crushing procedure (5 min), the grain sizes (1 mm to several ìm), and the diffusion coefficient for helium (cf., Section 2). Moreover, the corresponding neon isotopic compositions are inconsistent with a significant contribution of cosmogenic neon. Increasing R/R_a is accompanied by increasing ^{20}Ne/^{22}Ne together with increasing ^{21}Ne/^{22}Ne, which contrasts with the expected decreasing ^{20}Ne/^{22}Ne due to cosmogenic contamination, as observed for example in [80]. The results for sample AG99-36b that were acquired with particularly efficient crushing (600 strokes), compared to sample AG99-36c (400 strokes), are also characterized by ^{4}He similar to sample a (200 strokes) and ^{3}He between a and c (200 and 400 strokes). Finally, for sample AG99-35, increasing the stroke number from 200 to 325 (35a and 35b) did not influence the helium isotopic composition, despite the fact that radiogenic helium is unambiguously present in the sample matrix, as shown by the heating results (Table 1). Thus the quality of crushing clearly does not influence the contribution of cosmogenic and radiogenic helium in the samples from this study. Finally, contamination of the magmatic signature by cosmogenic and radiogenic signals from the matrix does not explain the compositional variability. In conclusion, the isotopic variations observed between duplicates are most likely related to the natural compositional variation of olivine in the samples. The detailed analysis of duplicates, and the results obtained by crushing and heating show that we cannot completely exclude a possible contribution of post-magmatic helium. However, such a contribution appears to be minor if any, and does not affect the major conclusions reached from this study (to follow).

4.2. Helium loss in olivine phenocrysts

Almost all of the Kerguelen samples are characterized by lower ^{4}He/^{21}Ne* (radiogenic/nucleogenic production ratio) and ^{3}He/^{22}Ne$_s$ (ratio corrected for air using a solar ^{20}Ne/^{22}Ne$=13.8$) than production and solar values [38,40] (Fig. 4). These ratios are particularly low for the Kerguelen Archipelago xenoliths [52] and have been interpreted as reflecting syn- or post-magmatic helium loss due to simple helium diffusion. The fact that the samples are distributed along a linear trend in Fig. 4 indeed suggests natural diffusion of helium. According to [52], because the xenolith correlation line passes through zero and solar/production ratios, this implies that the helium loss event is likely to be relatively recent, otherwise in-growth of radiogenic ^{4}He would have led to a systematic horizontal shift of the data. The same conclusion can be reached for the samples from this study, although with a lesser degree of helium loss as the olivine samples are closer to the solar and production ratios. Note that two samples have more radiogenic helium isotopic compositions compared to mantle values, which is consistent with the addition of radiogenic ^{4}He for these two samples.

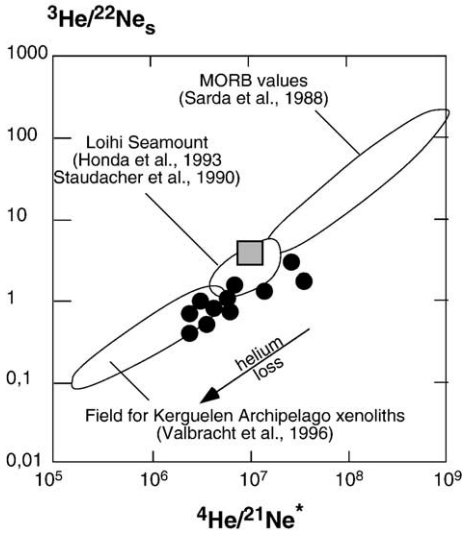

Fig. 4. $^3He/^{22}Ne_s$ vs. $^4He/^{21}Ne^*$. $^3He/^{22}Ne_s$ is the $^3He/^{22}Ne$ corrected for air-contamination (i.e., extrapolated to value of $^{20}Ne/^{22}Ne$ of 13.8 relative to air). The grey square represents the production ratio of radiogenic helium to nucleogenic neon ($^4He/^{21}Ne^*$) and the solar $^3He/^{22}Ne$ value (10^7; 3.6; [43,68]). Fields for typical oceanic island basalts (OIB, e.g., Loihi) and mid-ocean ridge basalts (MORB) are reported. The fields for Kerguelen Archipelago xenoliths show values significantly lower than mantle and this has been interpreted as reflecting helium loss during or after magmatic processes. The generally low values of $^3He/^{22}Ne_s$ vs. $^4He/^{21}Ne^*$ for the studied high-MgO basalts together with a slope that does not pass through zero suggest that helium loss may have been perturbed by addition of radiogenic ^4He (see explanation in the text).

4.3. Origin of the Kerguelen Archipelago basalts

The neon isotopic compositions of the studied samples show a clear anomaly compared to air (higher $^{20}Ne/^{22}Ne$ and $^{20}Ne/^{22}Ne$), reflecting a mantle-derived component (cf., Section 3.2). In addition, all of the neon isotopic results for Kerguelen Archipelago basalts are distributed linearly on a line characterized by a slope that is intermediate between the MORB and Iceland lines. This is in agreement with the moderate helium isotopic ratios observed in the Kerguelen basalts, between MORB and OIB values (cf., Sections 1 and 3.1). The Kerguelen line in the Ne isotopes diagram (Fig. 3) and the $^4He/^3He$ ratio lower than MORB values (Fig. 2) clearly suggest that the Kerguelen hotspot belongs to the family of primitive hotspots, such as Iceland and Hawaii. However below, we discuss the origin of moderate helium and neon isotopic ratios (between MORB and OIB). In Fig. 5, the $^{21}Ne/^{22}Ne$ extrapolated (corrected for air contamination; [65]) vs. helium isotopic compositions for the studied MgO-rich rocks are reported. Theoretical binary mixing curves between MORB and solar end-members are also indicated with r parameters ($r=(^3He/^{22}Ne)_{MORB}/(^3He/^{22}Ne)_{solar}$) of 1 and 10. Also reported are compositions for basalts from Loihi and Iceland [46,55,65–67], which define a global mixing trend between MORB and solar end-members. On this diagram, some of the Kerguelen Archipelago samples are distributed along the mixing curve between MORB and solar, and other samples are characterized by higher $^4He/^3He$ for a given $^{21}Ne/^{22}Ne$ extrapolated (e.g., sample AG99-35, 37 and 38). As explained in Section 4.1, compositional variations between duplicates, and heating results for AG99-35, AG99-37 and AG99-38 are inconsistent with significant post-magmatic radiogenic helium contribution during crushing, thus higher $^4He/^3He$ in these three samples reflects higher magmatic $^4He/^3He$. An important characteristic to consider is that the picrites (AG99-34, 36, 125, 126) have distinctly lower U (average $=0.4\pm0.1$ ppm) and Th (average $=1.75\pm0.25$ ppm) concentrations compared to those of the other MgO-rich basalts (AG99-35, 37, 38, 41) with values of U and Th of 0.9 ± 0.05 ppm and 4.05 ± 0.5 ppm, respectively [14]. This indicates that the picrites were generated from a source with lower U and lower Th than the other MgO-rich rocks. Therefore, the observation that the picrites are characterized by

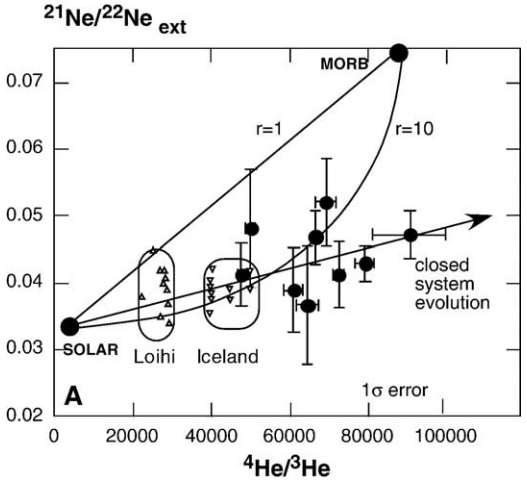

Fig. 5. $^{21}Ne/^{22}Ne$ extrapolated vs. measured $^4He/^3He$ in high-MgO basalts from the Kerguelen Archipelago. Two different binary mixing models between a MORB and a primitive mantle source are shown, and they are characterized by different values of r ($r=((^3He/^{22}Ne)_{MORB})/((^3He/^{22}Ne)_{solar\ or\ Loihi})=1$ or 10. The high-MgO basalts are generally distributed along the binary mixing lines between a plume-like source and MORB-like source, which is inconsistent with previously published data from [14]. Several samples have more radiogenic helium isotopic ratios (higher $^4He/^3He$) and the general distribution of the samples suggests that the source for the Kerguelen high-MgO basalts evolved in a relatively closed system from a (U, Th)/^3He-enriched source compared to the Iceland and Loihi sources.

higher magmatic R/R_a (lower $^4He/^3He$) is consistent with the hypothesis of a source having a lower (U+Th)/He. If we consider mixing as a possible mechanism for the variations of helium and neon, especially in the case of samples having lower U and Th concentrations, this may suggests that the Kerguelen source contains primitive material mixed with MORB-like material, leading to a relatively constant $^{21}Ne/^{22}Ne$ extrapolated value of ≈ 0.044 for the Kerguelen basalts (cf., Kerguelen line in Fig. 3).

Another hypothesis may explain the distribution of the samples in Fig. 5. The Kerguelen samples may have been derived from a source having initial solar helium and neon isotopic ratios of $^3He/^{22}Ne$ ~3 [43,68] and higher (U, Th)/^{3}He ratios compared to the Iceland and Hawaii plume sources. This source could have been isolated from the rest of the mantle, thus explaining the more radiogenic helium isotopic values that characterize the Kerguelen hotspot basalts (Fig. 5). This hypothesis is in agreement with the conclusions based on radiogenic isotope systematics [14], where the Sr–Pb isotopic systematics in the picrites and high-MgO basalts are clearly inconsistent with mixing of magmas derived from the enriched Kerguelen plume end-member and magmas derived from a MORB-like source.

The linear distribution of Kerguelen samples in the neon diagram (Fig. 3) clearly reflects an important air contamination of the samples. Air addition is a recurrent problem in noble gas geochemistry and the process for this air "contamination" is still debated (e.g., [69–72]). It may reflect a recycled air-like contaminant that has been preserved during subduction processes [72], undegassed mantle [73], syn- or post-eruptive atmospheric contamination [70]. An important observation for the studied high-MgO basalts is that low $^{20}Ne/^{22}Ne$ and low $^4He/^3He$ ratios are associated with higher $^{176}Hf/^{177}Hf$ ratios (reverse correlations in Fig. 6A and B, respectively). This is also valid for $^{21}Ne/^{22}Ne$ ratios that are correlated with $^{20}Ne/^{22}Ne$ ratios (cf., Fig. 3). Note that the range of $^{176}Hf/^{177}Hf$ ratios observed in Fig. 6 corresponds to the range defined for the enriched Kerguelen plume end-member [11,14,21]. Such reverse correlations have no direct chemical signification since Hf behavior is independent from neon and helium behavior, i.e., high $^{176}Hf/^{177}Hf$ does not reflect atmospheric contamination, contrary to low $^{20}Ne/^{22}Ne$ and $^{21}Ne/^{22}Ne$. However, the observation that high $^{176}Hf/^{177}Hf$ is associated with low $^{20}Ne/^{22}Ne$ and $^{21}Ne/^{22}Ne$ and low $^4He/^3He$ is real. This indicates that the source characterized by higher $^{176}Hf/^{177}Hf$ is primitive with respect to its helium isotopic composition, and has been air-contaminated,

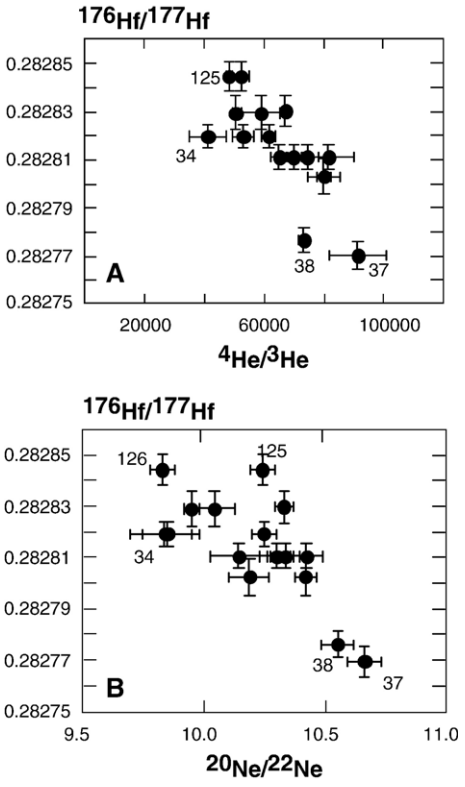

Fig. 6. $^{176}Hf/^{177}Hf$ vs. $^4He/^3He$ (A) and $^{176}Hf/^{177}Hf$ vs. $^{20}Ne/^{22}Ne$ (B) for the olivines from high-MgO basalts on the Kerguelen Archipelago. The results show that $^4He/^3He$ and $^{20}Ne/^{22}Ne$ are reversely correlated with $^{176}Hf/^{177}Hf$. This suggests that the air-like contaminant, which is reflected in the lower $^{20}Ne/^{22}Ne$ values (because of a nearly constant $^{21}Ne/^{22}Ne_{ext}$, cf., Fig. 3), is characterized by the most primitive $^4He/^3He$ compositions (highest R/R_a), and by the most radiogenic Hf, characteristics of the enriched Kerguelen plume end-member [21].

as shown by neon isotopic compositions. This is an important result that has not been observed before and clearly confirms the conclusions reached in Section 4.1 that helium and neon isotopic compositions measured in the samples reflect magmatic compositions with no significant contribution of post-magmatic cosmogenic and/or radiogenic helium. In addition, $^4He/^3He$ and Ne isotopic ratios are slightly correlated with Nd isotopic ratios (not shown), and generally helium and neon isotopic variations from the samples in this study are not correlated with other isotopic system (Pb, Sr). These observations are not problematic, because [14] show that Hf isotopic variations observed in the studied basalts also appear to be decoupled from $^{206}Pb/^{204}Pb$ variations (e.g., Fig. 15 in [14]). These authors interpreted the Hf isotopic variations as reflecting discrete heterogeneities in the Kerguelen mantle plume itself. Finally, the comparison of the helium and neon isotopic

results with Hf isotopic variations in these samples [14] place some important constraints on the nature of the discrete components present within the plume. The observed variations suggest that the air-like contaminant, which is reflected in the lower $^{20}Ne/^{22}Ne$ values (because of a nearly constant $^{21}Ne/^{22}Ne_{ext}$, cf., Fig. 3), is characterized by most primitive $^{4}He/^{3}He$ compositions (highest R/R_a), and by the most radiogenic Hf. Below, we evaluate two different hypotheses that could account for the observed rare gas isotopic vs. Hf isotopic ratio correlation: (1) assimilation of the overlying Cretaceous Kerguelen Plateau during magma ascent through the lithosphere, or (2) recycling of an atmospheric neon-like end-member within the Kerguelen plume source.

Possible contamination of the high-MgO parental magmas from the studied basalts by the overlying northern Kerguelen Plateau can be evaluated by examining the compositional characteristics of the plateau. The northern Kerguelen Plateau basalts [77] that could have potentially contaminated the high-MgO magmas have higher $^{176}Hf/^{177}Hf$ than estimates for the Kerguelen plume ($Hf_i>6$; [14]), with evidence for binary mixing between the SEIR–MORB source and the enriched Kerguelen plume source [11]. Therefore, this part of the Kerguelen Plateau should be characterized by helium isotopic ratios that are intermediate between MORB ratios and primitive ratios observed in many hotspots formed by melting of a deep-seated mantle plume (e.g., [74–76]). They should also be characterized by atmospheric neon isotopic composition, due to syn-eruption neon contamination of lavas forming the Kerguelen Plateau. However, the MgO-rich rocks are slightly shifted to lower Hf isotopic ratios compared to other Kerguelen basalts ($Hf_i<4$; [14]) and if they were contaminated by the Kerguelen Plateau during ascent, we may expect higher $^{176}Hf/^{177}Hf$ ratios than those observed. Some Cretaceous Kerguelen Plateau lavas (Site 1137) have distinctly lower $^{176}Hf/^{177}Hf$ than estimates for the Kerguelen plume [11], as observed for the high-MgO basalts from the Aubert de la Rüe area (Fig. 1). However, these plateau basalts are located almost 10° to the south of the Kerguelen Archipelago at Elan Bank (western salient of the southern Kerguelen Plateau). There is no direct evidence of the MgO-rich basalts being contaminated by the Kerguelen Plateau, because there are no appropriate compositions recorded to date on the Kerguelen Plateau that could account for the compositions of the studied MgO-rich rocks (cf., discussion in [14]).

Below we evaluate the hypothesis of recycling of an atmospheric neon-like end-member within the Kerguelen plume source. It has been shown that the studied high-MgO basalts have Sr–Nd isotopic compositions typical of the enriched composition of the Kerguelen plume [14]. The high-MgO basalts located near the Mt. Ross volcano, on the Aubert de la Rüe Peninsula (Fig. 1) are characterized by slightly lower $^{176}Hf/^{177}Hf$ (≈ 0.28275) compared to basalts located in Armor and on the Courbet Peninsula whose compositions are comparable to those for the enriched component of the Kerguelen plume with $^{176}Hf/^{177}Hf \approx 0.28285$ [21]. These slight differences have been interpreted as potentially reflecting small-scale heterogeneities present within the Kerguelen plume itself [14]. The fact that higher $^{176}Hf/^{177}Hf$ in Fig. 6 are associated with lower $^{20}Ne/^{22}Ne$ and $^{4}He/^{3}He$ clearly indicates that air-like contamination (lower $^{20}Ne/^{22}Ne$) increases with an increasing contribution of the more primitive helium component (lower $^{4}He/^{3}He$), and with sampling of the composition of the Kerguelen plume recorded on the Courbet Peninsula with $^{176}Hf/^{177}Hf \approx 0.28285$. The part of the Kerguelen plume characterized by lower $^{176}Hf/^{177}Hf$, which is recorded in sample AG99-37 and -38 for example, is also characterized by primitive $^{21}Ne/^{22}Ne_{ext}$ values (0.047 and 0.041, respectively), in agreement with a deep mantle plume origin, but is also characterized by MORB-like $^{4}He/^{3}He$ values (Fig. 6). Thus the most radiogenic helium isotopic compositions recorded in the studied basalts are inconsistent with a MORB-like source origin, in agreement with the conclusions of the trace element and radiogenic isotope study from [14]. These observations further suggest that the high-MgO basalts were generated from a heterogeneous mantle source characterized by variable initial $(U,Th)/^{3}He$ ratios. The He–Ne–Hf systematics suggest that the part of this source, which may have higher initial $(U,Th)/^{3}He$, was less contaminated by an atmosphere-like component.

5. Summary and conclusions

Important variations of helium isotopic compositions are observed in basalts from the Kerguelen Archipelago. The $^{4}He/^{3}He$ ratios vary from typical MORB values to more primitive ratios observed in OIB ($^{4}He/^{3}He$ ~41,218; $R/R_a=17.5$). This variability is mostly related to the natural variability of magmatic olivine signatures within individual samples. A minor contribution of cosmogenic and radiogenic helium accumulated in the matrix during exposure time cannot be excluded but combined crushing and heating extraction procedures for gas analysis allowed us to consider results obtained by crushing as reflecting

magmatic compositions and to conclude that the Kerguelen samples are mostly characterized by a primitive helium isotopic composition. The nearly constant and primitive mantle $^{21}Ne/^{22}Ne_{corrected\ for\ air\ contamination}$ value of ≈ 0.044 confirms the deep mantle source origin of the high-MgO basalts and indicates source characteristics that are intermediate between MORB and Iceland values. The source of the Kerguelen Archipelago basalts could be a homogeneous mixture between a MORB-like source and a primitive/solar-like lower mantle source, but this hypothesis is inconsistent with detailed He–Ne systematics and with previously published Sr–Nd–Hf–Pb isotopic systematics. The primitive characteristics of the Kerguelen basalts are consistent with a deep mantle plume origin. However, generally lower and variable $^{4}He/^{3}He$ helium and higher $^{21}Ne/^{22}Ne_{corrected\ for\ air\ contamination}$ compared to other OIB such as Iceland suggest that the Kerguelen hotspot source is generally heterogeneous and is mostly characterized by initial $(U,Th)/^{3}He$ ratios that are higher compared to the Iceland plume source and may have evolved in a relatively closed system.

Acknowledgments

We are grateful to the captains and crews of the Marion Dufresne II and La Curieuse, the IPEV, and the TAAF for logistical support during the CartoKer 1999/2000 mapping program. We thank M. Kurz from the Woods Hole Oceanographic Institution for carrying out the duplicate helium analyses. We are grateful to the two anonymous reviewers, whose useful comments helped us to clarify some important aspects of the paper. This work was partly supported by an ARC grant (ARC 98/03-233; Actions de Recherches Concertées from the Communauté Française de Belgique).

References

[1] F.A. Frey, N.J. McNaughton, D.R. Nelson, J.R. DeLaeter, R.A. Duncan, Petrogenesis of the Bunbury Basalts, western Australia: interaction between the Kerguelen plume and Gondwana lithosphere? Earth Planet. Sci. Lett. 144 (1996) 163–183.

[2] J.J. Mahoney, W.B. Jones, F.A. Frey, V.J.M. Salters, D.G. Pyle, H.L. Davies, Geochemical characteristics of lavas from Broken Ridge, the Naturaliste Plateau and southernmost Kerguelen plateau: Cretaceous plateau volcanism in the southeast Indian Ocean, Chem. Geol. 120 (1995) 315–345.

[3] R.W. Kent, M.P. Pringle, R.D. Müller, A.D. Saunders, $^{40}Ar/^{39}Ar$ geochronology of the Rajmahal basalts, India, and their relationship to the Kerguelen Plateau, J. Petrol. 43 (2002) 1141–1153.

[4] R.W. Kent, A.D. Saunders, P.D. Kempton, N.C. Ghose, Rajmahal basalts, Eastern India: mantle sources and melt distribution at a volcanic rifted margin, in: J.J. Mahoney, M.F. Coffin (Eds.), Large Igneous Provinces: Continental, Oceanic, and Planetary Flood Volcanism, Geophysical Monograph, vol. 100, AGU, Washington, 1997, pp. 145–182.

[5] S. Ingle, D. Weis, J. Scoates, F.A. Frey, Relationship between the early Kerguelen plume and continental flood basalts of the paleo-eastern Gondwanan margins, Earth Planet. Sci. Lett. 197 (2002) 35–50.

[6] F.A. Frey, D. Weis, Temporal evolution of the Kerguelen plume: geochemical evidence from ~38 to 82 Ma lavas forming the Ninetyeast Ridge, Contrib. Mineral. Petrol. 121 (1995) 12–28.

[7] F.A. Frey, M.F. Coffin, P.J. Wallace, D. Weis, X. Zhao, S.W. Wise Jr., V. Wähnert, D.A.H. Teagle, P.J. Saccocia, D.N. Reusch, M.S. Pringle, K.E. Nicolaysen, C.R. Neal, R.D. Müller, C.L. Moore, J.J. Mahoney, L. Keszthelyi, H. Inokuchi, R.A. Duncan, H. Delius, J.E. Damuth, D. Damasceno, H.K. Coxall, M.K. Borre, F. Boehm, J. Barling, N.T. Arndt, M. Antretter, Origin and evolution of a submarine large igneous province: the Kerguelen Plateau and Broken Ridge, southern Indian Ocean, Earth Planet. Sci. Lett. 176 (2000) 73–89.

[8] F.A. Frey, D. Weis, A.Y. Borisova, G. Xu, Involvement of continental crust in the formation of the Cretaceous Kerguelen Plateau: new perspectives from ODP Leg 120 sites, J. Petrol. 43 (2002) 1207–1239.

[9] D. Weis, F.A. Frey, A. Saunders, I. Gibson, and Leg 121 Shipboard Scientific Party, Ninetyeast Ridge (Indian Ocean): a 5000 km record of a Dupal mantle plume, Geology 19 (1991) 99–102.

[10] S. Ingle, D. Weis, F.A. Frey, Indian continental crust recovered from Elan Bank, Kerguelen Plateau (ODP Leg 183, site 1137), J. Petrol. 43 (2002) 1241–1257.

[11] S. Ingle, D. Weis, S. Doucet, N. Mattielli, Hf isotope constraints on mantle sources and shallow-level contaminants during Kerguelen hot spot activity since ~120 Ma, Geochem. Geophys. Geosyst. 4 (2003) (2002GC000482).

[12] D. Weis. Role of the Kerguelen Plume in the geochemical evolution of the Indian Ocean mantle, Habilitation thesis, Université Libre de Bruxelles, 1992.

[13] S. Doucet, D. Weis, J. Scoates, K. Nicolaysen, F. Frey, A. Giret, Petrogenesis of high- and low-MgO transitional basalts from the Loranchet Peninsula (Mont des Ruches and Mont Fontaine), Kerguelen Archipelago, J. Petrol. 43 (2002) 1341–1366.

[14] S. Doucet, J.S. Scoates, D. Weis, A. Giret, Constraining the components of the Kerguelen mantle plume: a Hf–Pb–Sr–Nd isotopic study of picrites and high-MgO basalts from the Kerguelen Archipelago, Geochem. Geophys. Geosyst. 6 (2005) (2004GC000806).

[15] I. Gautier, D. Weis, J.-P. Mennessier, P. Vidal, A. Giret, M. Loubet, Petrology and geochemistry of Kerguelen basalts (South Indian Ocean): evolution of the mantle sources from ridge to an intraplate position, Earth Planet. Sci. Lett. 100 (1990) 59–76.

[16] Y.J. Yang, F.A. Frey, D. Weis, A. Giret, D. Pyle, G. Michon, Petrogenesis of the flood basalts forming the northern Kerguelen Archipelago: implications for the Kerguelen Plume, J. Petrol. 39 (4) (1998) 711–748.

[17] J.J. Mahoney, J.D. McDougall, G.W. Lugmair, K. Gopalan, Kerguelen hot spot source for the Rajmahal traps and Ninetyeast Ridge, Nature 303 (1983) 385–389.

[18] F.A. Frey, K. Nicolaysen, B.K. Kubit, D. Weis, A. Giret, Flood basalts from Mont Tourmente in the central Kerguelen Archipelago: the change from tholeiitic/transitional to alkali basalts at ~25 Ma, J. Petrol. 43 (2002) 1367–1387.
[19] D. Weis, F.A. Frey, H. Leyrit, I. Gautier, Kerguelen Archipelago revisited: geochemical and isotopic study of the SE Province lavas, Earth Planet. Sci. Lett. 118 (1993) 101–119.
[20] D. Weis, F.A. Frey, A. Giret, J.-M. Cantagrel, Geochemical characteristics of the youngest volcano (Mount Ross) in the Kerguelen Archipelago: inferences for magma flux and composition of the Kerguelen plume, J. Petrol. 39 (1998) 973–994.
[21] N. Mattielli, D. Weis, J. Blichert-Toft, F. Albarède, Hf isotope evidence for a Miocene change of regime of the Kerguelen hot spot, J. Petrol. 43 (7) (2002) 1327–1339.
[22] D. Weis, D. Damasceno, F.A. Frey, K. Nicolaysen, A. Giret, Temporal isotopic variations in the Kerguelen plume: evidence from the Kerguelen Archipelago, Mineralogical Magazine 62A (Goldschmidt Conference Toulouse 1998), 1998, pp. 1643–1644.
[23] D. Weis, F.A. Frey, R. Schlich, M. Schaming, R. Montigny, D. Damasceno, N. Mattielli, K. Nicolaysen, J. Scoates, Trace of the Kerguelen mantle plume: evidence from seamounts between the Kerguelen Archipelago and Heard Island, Indian Ocean, Geochem. Geophys. Geosyst. (2002), doi:10.1029/2001GC000251.
[24] C.J. Allègre, Isotope geodynamics, Earth Planet. Sci. Lett. 86 (1987) 175–203.
[25] C.J. Allègre, M. Moreira, T. Staudacher, $^{4}He/^{3}He$ dispersion and mantle convection, Geophys. Res. Lett. 22 (17) (1995) 2325–2328.
[26] D.W. Graham, S.E. Humphris, W.J. Jenkins, M.D. Kurz, Helium isotope geochemistry of some volcanic rocks from Saint Helena, Earth Planet. Sci. Lett. 110 (1993) 121–131.
[27] D.R. Hilton, K. Grönvold, C. Macpherson, P.P. Castillo, Extreme $^{3}He/^{4}He$ ratios in northwest Iceland: constraining the common component in mantle plumes, Earth Planet. Sci. Lett. 173 (1999) 53–60.
[28] D.R. Hilton, C.G. Macpherson, T.R. Elliott, Helium isotope ratios in mafic phenocrysts and geothermal fluid from La Palma, the Canary Islands (Spain): implications for HIMU mantle sources, Geochim. Cosmochim. Acta 64 (2000) 2119–2132.
[29] M.D. Kurz, W.J. Jenkins, S.R. Hart, Helium isotopic systematics of oceanic islands and mantle heterogeneity, Nature 297 (1982) 43–47.
[30] M. Moreira, R. Doucelande, M.D. Kurz, B. Dupré, C.J. Allègre, Helium and lead isotope geochemistry of the Azores Archipelago, Earth Planet. Sci. Lett. 169 (1999) 189–205.
[31] M. Moreira, M.D. Kurz, Subducted oceanic lithosphere and the origin of the 'high μ' basalt helium isotopic signature, Earth Planet. Sci. Lett. 189 (2001) 49–57.
[32] F.M. Stuart, S. Lass-Evans, J.G. Fitton, R.M. Ellam, High $^{3}He/^{4}He$ ratios in picritic basalts from Baffin Island and the role of a mixed reservoir in mantle plumes, Nature 424 (2003) 57–59.
[33] C.J. Allègre, M. Moreira, Rare gas systematics and the origin of oceanic islands: the key role of entrainment at the 670 km boundary layer, Earth Planet. Sci. Lett. 228 (2004) 85–92.
[34] A. Zindler, S. Hart, Helium: problematic primordial signals, Earth Planet. Sci. Lett. 79 (1986) 1–8.
[35] C. Class, S. Goldstein, M. Stute, M.D. Kurz, P. Schlosser, Grand Comore island: a well-constrained "low $^{3}He/^{4}He$" mantle plume, Earth Planet. Sci. Lett. 233 (2005) 391–409.
[36] D.R. Hilton, J. Barling, G.E. Wheller, Effect of shallow-level contamination on the helium isotope systematics of ocean-island lavas, Nature 373 (1995) 330–333.
[37] M. Moreira, C.J. Allègre, Helium isotopes on the Macdonald seamount (Austral chain): constraints on the origin of the superswell, C.R. Géosci. 336 (2004) 983–990.
[38] I. Yatsevich, M. Honda, Production of nucleogenic neon in the Earth from natural radioactive decay, J. Geophys. Res. 102 (1997) 10291–10298.
[39] P. Sarda, T. Staudacher, C. Allègre, Neon isotopes in submarine basalts, Earth Planet. Sci. Lett. 91 (1988) 73–88.
[40] J.-P. Benkert, H. Baur, P. Signer, R. Wieler, He, Ne and Ar from the solar wind and solar energetic particles in lunar ilmenites and pyroxenes, J. Geophys. Res. 98 (1993) 13147–13162.
[41] E. Dixon, M. Honda, I. McDougall, I. Campbell, I. Sigurdsson, Preservation of near-solar neon isotopic ratios in Icelandic basalts, Earth Planet. Sci. Lett. 180 (2000) 309–324.
[42] M. Honda, I.I. McDougall, D.B. Patterson, A. Doulgeris, D. Clague, Noble gases in submarine pillow basalt glasses from Loihi and Kilauea, Hawaii: a solar component in the Earth, Geochim. Cosmochim. Acta 57 (1993) 859–874.
[43] M. Honda, I. McDougall, D.B. Patterson, A. Doulgeris, D.A. Clague, Possible solar noble-gas component in Hawaiian basalts, Nature 349 (1991) 149–151.
[44] P. Madureira, M. Moreira, J. Mata, C.J. Allègre, Primitive helium and neon isotopes in Terceira Island (Azores archipelago), Earth Planet. Sci. Lett. 233 (2005) 429–440.
[45] M. Moreira, C.J. Allègre, Helium–neon systematics and the structure of the mantle, Chem. Geol. 147 (1998) 53–59.
[46] M. Moreira, K. Breddam, J. Curtice, M.D. Kurz, Solar neon in the Icelandic mantle: new evidence for an undegassed lower mantle, Earth Planet. Sci. Lett. 185 (2001) 15–23.
[47] R.J. Poreda, K.A. Farley, Rare gases in Samoan xenoliths, Earth Planet. Sci. Lett. 113 (1992) 129–144.
[48] M. Trieloff, J. Kunz, D.A. Clague, D. Harrison, C.J. Allègre, The nature of pristine noble gases in mantle plumes, Science 288 (2000) 1036–1038.
[49] R. Pepin, On the origin and early evolution of terrestrial planet atmospheres and meteoritic volatiles, Icarus 92 (1991) 2–79.
[50] R.O. Pepin, Evolution of Earth's noble gases: consequences of assuming hydrodynamic loss driven by giant impact, Icarus 126 (1997) 148–156.
[51] T. Trull, S. Nadeau, F. Pineau, M. Polvé, M. Javoy, C–He systematics in hotspot xenoliths: implications for mantle carbon contents and carbon recycling, Earth Planet. Sci. Lett. 118 (1993) 43–64.
[52] P.J. Valbracht, M. Honda, T. Matsumoto, N. Mattielli, I. McDougall, R. Ragettli, D. Weis, Helium, neon and argon isotope systematics in Kerguelen ultramafic xenoliths: implications for mantle source signatures, Earth Planet. Sci. Lett. 138 (1996) 29–38.
[53] D. Vance, J.O.H. Stone, R.K. O'Nions, He, Sr and Nd isotopes in xenoliths from Hawaii and other oceanic islands, Earth Planet. Sci. Lett. 96 (1989) 147–160.
[54] E.T. Dixon, Interpretation of helium and neon isotopic heterogeneity in Icelandic basalts, Earth Planet. Sci. Lett. 206 (2003) 83–99.
[55] P.J. Valbracht, T. Staudacher, A. Malahoff, C.J. Allègre, Noble gas systematics of deep rift zone glasses from Loihi Seamount, Hawaii, Earth Planet. Sci. Lett. 150 (1997) 399–411.

[56] M.D. Kurz, Cosmogenic helium in a terrestrial igneous rock, Nature 320 (1986) 435–439.
[57] P. Sarda, T. Staudacher, C.J. Allègre, A. Lecomte, Cosmogenic neon and helium at Réunion: measurement of erosion rate, Earth Planet. Sci. Lett. 119 (1993) 405–417.
[58] T. Staudacher, C.J. Allègre, Age of the second caldera of Piton de la Fournaise volcano, Réunion Island, determined by cosmic ray produced ^{3}He and ^{21}Ne, Earth Planet. Sci. Lett. 119 (1993) 395–404.
[59] T. Staudacher, C.J. Allègre, The cosmic ray produced ^{3}He/^{21}Ne ratio in ultramafic rocks, Geophys. Res. Lett. 20 (11) (1993) 1075–1078, doi:10.1029/93GL01244.
[60] P. Scarsi, Fractional extraction of helium by crushing of olivine and clinopyroxene phenocrysts: Effects on the ^{3}He/^{4}He measured ratio, Geochim. Cosmochim. Acta 64 (21) (2000) 3751–3762.
[61] R. Yokochi, B. Marty, R. Pik, P. Burnard, High ^{3}He/^{4}He ratios in peridotite xenoliths from SW Japan revisited: evidence for cosmogenic ^{3}He released by vacuum crushing, Geochem. Geophys. Geosyst. 6 (2005) Q01004, doi:10.1029/2004GC000836.
[62] K. Nicolaysen, F.A. Frey, K. Hodges, D. Weis, A. Giret, 40Ar/39Ar geochronology of flood basalts, from the Kerguelen Archipelago, southern Indian Ocean: Implications for Cenozoic eruption rates of the Kerguelen plume, Earth Planet. Sci. Lett. 174 (2000) 313–328.
[63] T.W. Trull, M.D. Kurz, Experimental measurements of ^{3}He and ^{4}He mobility in olivine and clinopyroxene at magmatic temperatures, Geochim. Cosmochim. Acta 57 (1993) 1313–1324.
[64] M.D. Kurz, J. Curtice, D.E.L. III, A. Solow, Rapid helium isotopic variability in Mauna Kea shield lavas from the Hawaiian Scientific Drilling Project, Geochem. Geophys. Geosyst. 5 (4) (2004) (2002GC000439).
[65] M. Moreira, T. Staudacher, P. Sarda, J.-G. Schilling, C.J. Allègre, A primitive plume neon component in MORB: the Shona ridge-anomaly, South Atlantic (51–52 °S), Earth Planet. Sci. Lett. 133 (1995) 367–377.
[66] M.D. Kurz, M. Moreira, J. Curtice, D.E. Lott III, J.J. Mahoney, J.M. Sinton, Correlated helium, neon, and melt production on the super-fast spreading East Pacific Rise near 17°S, Earth Planet. Sci. Lett. 232 (2005) 125–142.
[67] P. Sarda, M. Moreira, T. Staudacher, J.-G. Schilling, C.J. Allègre, Rare gas systematics on the southernmost mid-Atlantic Ridge: constraints on the lower mantle and the Dupal source, J. Geophys. Res. 105 (2000) 5973–5996.
[68] M. Ozima, F.A. Podosek, Noble Gas Geochemistry, Cambridge University Press, 1983.
[69] K.A. Farley, R.J. Poreda, Mantle neon and atmospheric contamination, Earth Planet. Sci. Lett. 114 (1993) 325–339.
[70] C. Ballentine, D. Bardford, The origin of air-like noble gases in MORB and OIB, Earth Planet. Sci. Lett. 180 (2000) 39–48.
[71] T. Matsumoto, Y. Chen, J. Matsuda, Concomitant occurrence of primordial and recycled noble gases in the Earth's mantle, Earth Planet. Sci. Lett. 185 (2001) 35–47.
[72] P. Sarda, Surface noble gas recycling to the terrestrial mantle, Earth Planet. Sci. Lett. 228 (2004) 49–63.
[73] C.J. Allègre, T. Staudacher, P. Sarda, M.D. Kurz, Constraints on evolution of Earth's 30 mantle from rare gas systematics, Nature 303 (1983) 762–766.
[74] V. Courtillot, A. Davaille, J. Besse, J. Stock, Three distinct types of hotspots in the Earth's mantle, Earth Planet. Sci. Lett. 205 (2003) 295–308.
[75] A. Davaille, Simultaneous generation of hotspots and superswells by convection in a heterogeneous planetary mantle, Nature 402 (1999) 756–760.
[76] A. Davaille, Two-layer thermal convection in miscible viscous fluids, J. Fluid Mech. 379 (1999) 223–253.
[77] D. Weis, F.A. Frey, Submarine basalts of the northern Kerguelen Plateau: interaction between the Kerguelen plume and the Southeast Indian Ridge revealed at ODP Site 1140, J. Petrol. 43 (2002) 1287–1309.
[78] J. Nougier, Carte géologique au 1/200000 de l'archipel des Kerguelen, Institut Géographique National, Paris, 1970.
[79] R.L. Palma, R.H. Becker, R.O. Pepin, D.J. Schlutter, Irradiation records in regolith materials, II: solar wind and solar energetic particle components in helium, neon, and argon extracted from single lunar mineral grains and from the Kapoeta howardite by stepwise pulse heating, Geochim. Cosmochim. Acta 66 (2002) 2929–2958.
[80] M. Moreira, P. Madureira, Cosmogenic helium and neon in 11 myr old ultramafic xenoliths: consequences for mantle signatures in old samples, Geochem. Geophys. Geosyst. 6 (2005) (1029/2005GC000939).